24th INTERNATIONAL CONGRESS ON SOUND AND VIBRATION
23–27 July 2017, London

# AEROELASTICITY OF A ROTATING BLADE COUPLED WITH A NONLINEAR ENERGY SINK

Hulun Guo, Shuqian Cao and Yushu Chen

*Tianjin University, Department of Mechanics, Tianjin, China*
*Tianjin Key Laboratory of Nonlinear Dynamics and Control, Tianjin, China*
*email: hlguo@tju.edu.cn*

In this paper, aeroelasticity of a rotating blade coupled with a nonlinear energy sink (NES) under supersonic flow is investigated. The bending and torsional of rotating blade is considered. The aerodynamic load is determined by first-order piston theory. The dynamic model of a rotating blade coupled with a NES is obtained. The Galerkin method is applied to discrete the nonlinear partial equations. Then, the dynamic responses of rotating blade are obtianed by numerical method. Results show that NES could mitigate the vibration of blade and change an aeroelastic instability blade to a stable blade. The flutter boundary of rotating blade is investigated by solving the eigenvalue problem. Lastly, the influences of NES parameters (mass, damping, nonlinear stiffness, and position of NES) on flutter boundary of rotating blade are investigated in detial.

Keywords: Rotating blade, NES, Aeroelasticity, Vibration suppression, Flutter

## 1. Introduction

Advanced rotating turbomachinery blades operate at high speed. As a result of the high speed airflow, static and dynamic instabilities can occur [1, 2]. Therefore, the ability to predict the aeroelastic behavior and suppress the aeroelastic response of such structural components becomes of great practical importance.

Librescu [3] and Oh [4, 5] showed that static and dynamic instabilities are induced by high speed airflow. Friedmann and Silverthorn [6] studied the stability of a helicopter blade in forward flight using multivariable Floquet-Liapunov theory. Friedmann and Yuan [7] modified strip theories, and applied in a coupled flap-lag-torsional aeroelastic analysis of the rotor blade in hover. Friedmann and Robinson [8] studied the incorporation of finite-state, time-domain aerodynamics in a flap-lag-torsional aeroelastic stability and response analysis in forward flight. Kim and Dugundji [9] investigated the nonlinear, large amplitude aeroelastic behavior of hingeless composite rotor blades during hover. Nonlinear stall aerodynamics was included by use of the ONERA airforces model. Jeon et al. [10] investigated the aeroelastic phenomena of a composite rotor blade in hover using a finite element method. The aerodynamic was modeled by a two-dimensional, quasi-steady strip theory.

Sinha [11] studied the dynamic response of a rotating cantilever twisted and inclined airfoil blade subjected to contact loads at the free end. Hansen [12] reviewed the major studies on aeroelastic instabilities of modern wind turbines and identified coupled mode flutter as a possible dynamic instability phenomenon for wind turbine blades operating in the attached flow regime. Pourazarm et al. [13] studied the influence of random lift of flow and random variation of the torsional natural frequency of the blade on the flutter of wind turbine blade. The influence of the natural frequencies in the torsional and flapwise directions on the critical flutter speed for wind turbine blade was also investigated [14].

Recently, Vakakis et al. [15] proposed a new nonlinear absorber named nonlinear energy sink (NES) which contained a linear damping, a nonlinear stiffness and a small mass. Georgiades and Vakakis[16] provided numerical evidence of targeted energy transfer from a linear flexible beam under shock excitation to a NES. Ahmadabadi and Khadem[17] investigated the bifurcations and topological structure of nonlinear normal modes of two types of coupled NES on energy suppression of a cantilever beam under shock excitation. Bab et al.[18] used a NES to mitigate vibration of a rotating beam under an external force. The Hopf bifurcation, saddle-node bifurcation and strongly modulated responses were found in this system. However, they only analyzed the first model response of the rotating beam.

In this paper, NES is used to suppress aeroelastic responses of a rotating blade under supersonic flow. The bending and torsional of rotating blade is considered. The aerodynamic load is determined by first-order piston theory. Galerkin method is applied to dispose the nonlinear dynamic model. Then, the dynamic responses of rotating blade are obtianed by numerical method. The flutter boundary of rotating blade is obtained by solving the eigenvalue problem. Lastly, the influences of NES parameters (mass, damping, nonlinear stiffness, and position of NES) on flutter boundary of rotating blade are investigated in detial.

## 2. Dynamic model

Consider a rotating blade coupled with a nonlinear energy sink, as shown in Fig. 1. The length of the blade is $L$, and $\rho$ is the blade density, $E$ is the Young's modulus, $G$ is the shear modulus of elasticity, $I$ is the bending moment of inertia, $J$ is the torsional stiffness constant, $A$ is the cross-sectional area, $K_m$ is the polar radius of gyration of the cross-section about the elastic axis, $K_{m1}$ and $K_{m2}$ are the mass radii of gyration about the major neutral axis and an axis perpendicular to the chord through the elastic axis, $e$ is the distance between the mass (and area) centroid and the elastic axis (mass offset), and $L_a$ and $M_a$ are the resultant lift force and pitching moment, respectively, due to the aeroelastic interactions. The rotating speed of the blade is $\omega$. The vibration of the blade in torsional and flapwise bending is considered in this paper. To suppress the vibration of the blade, a NES is fixed on the blade at $d$. The NES is a small mass $m$ coupled with the beam by a nonlinear stiffness $k_s$ and linear damping $c_s$. The displacement of this small mass in is $w_s$.

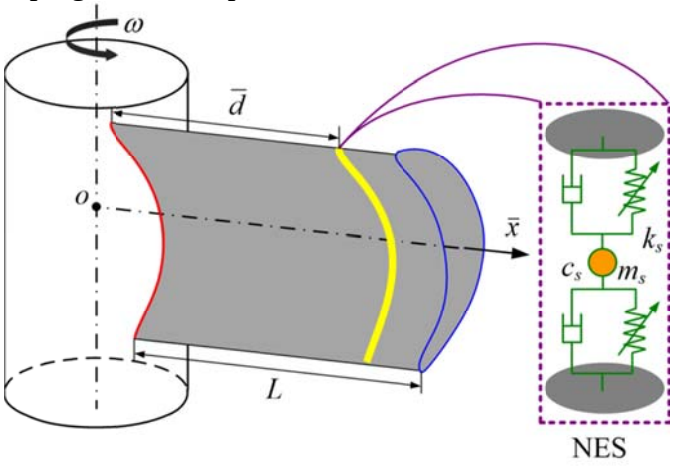


Figure 1: Rotating blade coupled with a NES.

The nonlinear aeroelastic equations of a rotating blade can be found in many literatures[13, 14], and the nonlinear equations of rotating beam coupled with a NES was obtained by Bab et al.[18]. Thus the governing equations of the rotating blade coupled with a NES can be written as:

$$
\begin{aligned}
&\rho A K_m^2 \frac{\partial^2 \varphi}{\partial t^2} + \rho A e \frac{\partial^2 w}{\partial t^2} - GJ \frac{\partial^2 \varphi}{\partial \bar{x}^2} - \frac{1}{2}\rho A \omega^2 (L^2 - \bar{x}^2)\left( K_m^2 \frac{\partial^2 \varphi}{\partial \bar{x}^2} + e \frac{\partial^2 w}{\partial \bar{x}^2} \right) \\
&+ \rho A \omega^2 \bar{x}\left( K_m^2 \frac{\partial \varphi}{\partial \bar{x}} + e \frac{\partial w}{\partial \bar{x}} \right) + \rho A \omega^2 \left( K_{m2}^2 - K_{m1}^2 \right)\varphi = M_a \\
&\rho A \frac{\partial^2 w}{\partial t^2} + \rho A e \frac{\partial^2 \varphi}{\partial t^2} + EI \frac{\partial^4 w}{\partial \bar{x}^4} - \frac{1}{2}\rho A \omega^2 (L^2 - \bar{x}^2)\left( e \frac{\partial^2 \varphi}{\partial \bar{x}^2} + \frac{\partial^2 w}{\partial \bar{x}^2} \right) \\
&+ \rho A \omega^2 \bar{x}\left( e \frac{\partial \varphi}{\partial \bar{x}} + \frac{\partial w}{\partial \bar{x}} \right) - \delta(\bar{x} - \bar{d})\left[ c_s \left( \frac{\partial w}{\partial t} - \frac{dw_s}{dt} \right) + k_s \left( w - w_s \right)^3 \right] = L_a \\
&m \frac{d^2 w_s}{dt^2} + c_s \left( \frac{dw_s}{dt} - \frac{\partial w(\bar{d}, t)}{\partial t} \right) + k_s \left( w_s - w(\bar{d}, t) \right)^3 = 0.
\end{aligned}
\tag{1}
$$

It is assumed that the blade is exposed to supersonic gas flow. First-order piston theory is used to evaluate the perturbed gas pressure. The unsteady aerodynamic lift $L_a$ and moment $M_a$ of a rotating blade are expressed as

$$
\begin{aligned}
L_a &= -2\rho_\infty c_\infty b\left( \frac{\partial w}{\partial t} - ae \frac{\partial \varphi}{\partial t} + U\varphi \right) \\
M_a &= 2\rho_\infty c_\infty aeb\left( \frac{\partial w}{\partial t} - ae \frac{\partial \varphi}{\partial t} + U\varphi \right).
\end{aligned}
\tag{2}
$$

where $\rho_a$ is the density of air, $U$ is the flow speed ($U = x\omega$ at each cross section), $b$ is the chord length, $a$ is the distance between the elastic axis and the mid-chord, divided by $e$.

It is convenient to introduce the following dimensionless parameters: $w = e\xi$, $w_s = e\xi_s$, $\bar{x} = Lx$, $t = \tau L^2 \sqrt{\frac{\rho A}{EI}}$, $\omega = \frac{\Omega}{L^2}\sqrt{\frac{EI}{\rho A}}$, $\gamma = \frac{L}{e}$, $\chi = \frac{K_m}{e}$, $\chi_2 = \frac{K_{m2}^2 - K_{m1}^2}{e^2}$, $\beta = \frac{GJ}{EI}$, $\mu = \frac{2\rho_\infty c_\infty b L^2}{\sqrt{\rho A EI}}$, $\varepsilon = \frac{m}{\rho A L}$, $\zeta = \frac{c_s L^2}{m}\sqrt{\frac{\rho A}{EI}}$, $\eta = \frac{k_s \rho A e^2 L^4}{mEI}$. In terms of these, the governing equations of the blade-NES system can be written:

$$
\begin{aligned}
&\chi^2 \frac{\partial^2 \varphi}{\partial \tau^2} + \frac{\partial^2 \xi}{\partial \tau^2} - \beta\gamma^2 \frac{\partial^2 \varphi}{\partial X^2} - \frac{1}{2}\Omega^2 (1 - X^2)\left( \chi^2 \frac{\partial^2 \varphi}{\partial X^2} + \frac{\partial^2 \xi}{\partial X^2} \right) \\
&+ \Omega^2 X\left( \chi^2 \frac{\partial \varphi}{\partial X} + \frac{\partial \xi}{\partial X} \right) + \chi_2 \Omega^2 \varphi = a\mu\left( \frac{\partial \xi}{\partial \tau} - a \frac{\partial \varphi}{\partial \tau} + \gamma\Omega X\varphi \right) \\
&\frac{\partial^2 \xi}{\partial \tau^2} + \frac{\partial^2 \varphi}{\partial \tau^2} + \frac{\partial^4 \xi}{\partial X^4} - \frac{1}{2}\Omega^2 (1 - X^2)\left( \frac{\partial^2 \varphi}{\partial X^2} + \frac{\partial^2 \xi}{\partial X^2} \right) + \Omega^2 X\left( \frac{\partial \varphi}{\partial X} + \frac{\partial \xi}{\partial X} \right) \\
&- \delta(X - d)\varepsilon\left[ \zeta\left( \frac{\partial \xi}{\partial \tau} - \frac{d\xi_s}{d\tau} \right) + \eta\left( \xi - \xi_s \right)^3 \right] = -\mu\left( \frac{\partial \xi}{\partial \tau} - a \frac{\partial \varphi}{\partial \tau} + \gamma\Omega X\varphi \right) \\
&\frac{d^2 \xi_s}{d\tau^2} + \zeta\left( \frac{d\xi_s}{d\tau} - \frac{\partial \xi(d, \tau)}{\partial \tau} \right) + \eta\left( \xi_s - \xi(d, \tau) \right)^3 = 0.
\end{aligned}
\tag{3}
$$

The Galerkin method can be used to discretize (3), which gives

$$\begin{aligned} \varphi &= \Psi(x)q_1(\tau) \\ \xi &= \Phi(x)q_2(\tau). \end{aligned} \tag{4}$$

where Ψ(x) and Φ(x) is the first model shape of the bending and twist of a blade, respectively. They can be written as:

$$\Psi(x) = \sqrt{2}\sin\frac{\pi x}{2}. \tag{5}$$

$$\Phi(x) = C_0\left[\sin\beta_0 x - \sinh\beta_0 x + \frac{\cos\beta_0 + \cosh\beta_0}{\sin\beta_0 - \sinh\beta_0}\left(\cos\beta_0 x - \cosh\beta_0 x\right)\right]. \tag{6}$$

Moreover, we introduce

$$\xi_s = \Phi(d)q_2(\tau) + q_3(\tau). \tag{7}$$

Substituting (4)-(7) into (3), and integrating over *x* from 0 to 1, yields

$$\begin{aligned} &\ddot{q}_1 + \left(a_{11} + a_{12}\Omega^2 + \mu a_{13}\Omega\right)q_1 + a_{14}q_2 + \mu a_{15}\dot{q}_1 + \mu a_{16}\dot{q}_2 + a_{17}\left(\zeta\dot{q}_3 + \eta q_3^3\right) = 0 \\ &\ddot{q}_2 + \left(a_{21} + a_{22}\Omega^2 + \mu a_{23}\Omega\right)q_1 + \left(a_{24} + a_{25}\Omega^2\right)q_2 + \mu a_{26}\dot{q}_1 + \mu a_{27}\dot{q}_2 \\ &\qquad + a_{28}\left(\zeta\dot{q}_3 + \eta q_3^3\right) = 0 \\ &\ddot{q}_3 + \Phi(d)\ddot{q}_2 + \zeta\dot{q}_3 + \eta q_3^3 = 0. \end{aligned} \tag{8}$$

where $a_{11} = -b_0\beta\gamma^2\int_0^1\Psi(x)\Psi''(x)dx$, $a_{12} = \chi_2 b_0 + \int_0^1\Psi(x)\left(\frac{1}{2}(x^2-1)\Psi''(x) + x\Psi'(x)\right)dx$, $a_{13} = -\gamma b_0(a+1)\int_0^1 x\Psi(x)\Psi(x)dx$, $a_{14} = -b_0\int_0^1\Psi(x)\Phi^{(4)}(x)dx$, $a_{15} = (a^2+a)b_0$, $a_{16} = -a_0b_0(a+1)$, $a_{17} = -\varepsilon b_0\Psi(d)$, $a_{21} = \beta\gamma^2 b_0\int_0^1\Phi(x)\Psi''(x)dx$, $a_{22} = -\chi_2 a_0 b_0$, $a_{23} = \gamma(\chi^2+a)b_0\int_0^1 x\Psi(x)\Phi(x)dx$, $a_{24} = \chi^2 b_0\int_0^1\Phi(x)\Phi^{(4)}(x)dx$, $a_{25} = \int_0^1\Phi(x)\left(\frac{1}{2}(x^2-1)\Phi''(x) + x\Phi'(x)\right)dx$, $a_{26} = -a_0b_0(a\chi^2 + a^2)$, $a_{27} = b_0(\chi^2+a)$, $a_{28} = \varepsilon b_0\chi^2\Phi(d)$, $a_0 = \int_0^1\Psi(x)\Phi(x)dx$, $b_0 = (\chi^2-1)^{-1}$.

Without NES, the discretized dynamic model of rotating blade with aerodynamic force is

$$\begin{aligned} &\ddot{q}_1 + \left(a_{11} + a_{12}\Omega^2 + \mu a_{13}\Omega\right)q_1 + a_{14}q_2 + \mu a_{15}\dot{q}_1 + \mu a_{16}\dot{q}_2 = 0 \\ &\ddot{q}_2 + \left(a_{21} + a_{22}\Omega^2 + \mu a_{23}\Omega\right)q_1 + \left(a_{24} + a_{25}\Omega^2\right)q_2 + \mu a_{26}\dot{q}_1 + \mu a_{27}\dot{q}_2 = 0 \end{aligned} \tag{9}$$

## 3. Dynamic responses

Dynamic responses of a rotating blade coupled with a NES in supersonic flow is investigated in this section. In order to reveal the vibration suppression of NES for rotating blade, responses of rotating blade without NES is also obtained.

The main parameters used in this paper are chosen as: $\rho$=4420kg/m$^3$, $E$=123GPa, $G$=248MPa, $L$=30cm, $b$=3cm, $e$=3mm, $I$=0.16mm$^3$, $J$=9.16mm$^3$, $A$=120mm$^2$, $K_m$=8.7mm, $K_{m1}$=1.2mm, $K_{m2}$=8.7mm, $a$=1, $\beta_0$=1.87, $\rho_\infty$=1.29kg/m$^3$, $c_\infty$=340m/s.

In order to suppress the dynamic response of blade due to supersonic flow, a NES is located on the blade. If we take $\varepsilon$ = 0.1, $\zeta$ = 0.5, $\eta = 10^4$ and $d$ = 0.9, the dynamic response of the blade can be obtained by solving (8) and (9). Figure 2(a) and 2(b) give the dynamic responses of blade when the

non-dimensional rotating speeds are 13 and 15. When NES is removed, the vibration of blade is damped to zero for Ω=13, and appears unstable for Ω=15 due to aeroelasticity. When NES is used, the vibration of blade is damped more quickly for Ω=13, and the unstable phenomenon is changed as stable Ω=15.

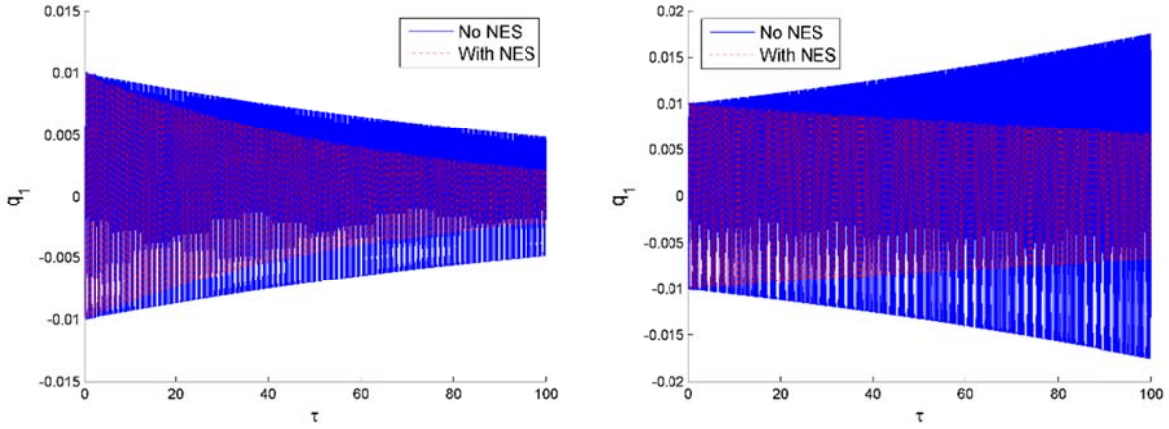


(a) Ω=13 (b) Ω=15

Figure 2: Dynamic response of rotating blade.

We can conclude that NES could mitigate the vibration of rotating blade and change unstable blade to stable blade. It means the flutter boundary of rotating blade is increased. In the following, we investigate the influences of NES parameters on the flutter boundary of rotating blade in detail.

## 4. Flutter boundary

In order to study the flutter boundary of rotating blade, we introduce

$$y = \{q_1 \quad \dot{q}_1 \quad q_2 \quad \dot{q}_2 \quad q_3 \quad \dot{q}_3\}^T \tag{10}$$

$$\overline{y} = \{q_1 \quad \dot{q}_1 \quad q_2 \quad \dot{q}_2\}^T \tag{11}$$

Then, (8) and (9) can be rewritten in matrix form.

$$\dot{y} = By + \eta y_5^3 \{0 \quad -a_{17} \quad 0 \quad -a_{28} \quad 0 \quad a_{28}\Phi(d) - 1\}^T \tag{12}$$

$$\dot{\overline{y}} = \overline{B}\overline{y} \tag{12}$$

Thus, the flutter boundary of rotating blade without NES can be solved according to the eigenvalue problem of (13), and the flutter boundary of rotating blade with a NES can be solved according to the eigenvalue problem of (12). In general the eigenvalues are complex. If the real of all eigenvalues are negative, the vibration of rotating blade is stable. If the real of one of the eigenvalues is positive, the rotating blade is unstable. Generally, the real of all eigenvalues of a rotating blade system are negative. As the rotating speed increased, the real of one of the eigenvalues of the rotating blade system may be positive. In this case, the rotating blade is aeroelastic instability. And the critical rotating speed is the flutter boundary of rotating blade.

If the main parameters are taken as section 3, and the non-dimensional parameters of NES are chosen as $\varepsilon = 0.1$, $\zeta = 0.5$, $\eta = 10^4$ and $d = 0.9$, the relationship between the real of all eigenvalues and the rotating speed is shown in Figure 3. When NES is removed, the flutter boundary of rotating blade is $\overline{\Omega}_f = 13.91$. When NES is used, the flutter boundary of rotating blade is $\Omega_f = 15.70$. Thus, the flutter boundary of rotating blade is increased evidently by NES.

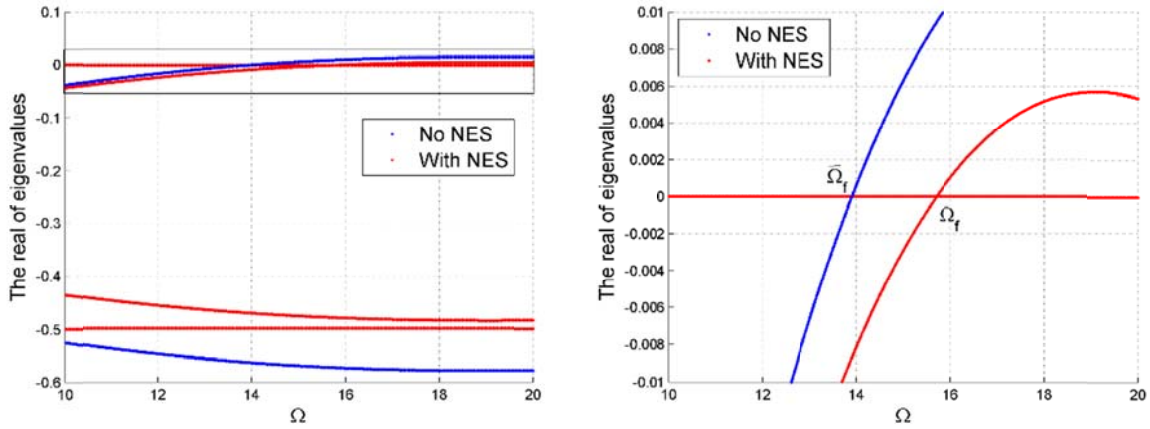


Figure 3: The real of all eigenvalues vs. rotating speed.

Figure 4 shows the relationship between the flutter boundary and NES mass ratio $\varepsilon$. It shows that increasing NES mass ratio $\varepsilon$ would increase the flutter boundary of a rotating blade. When NES mass is too small, NES could absorb few vibration energy from rotating blade.

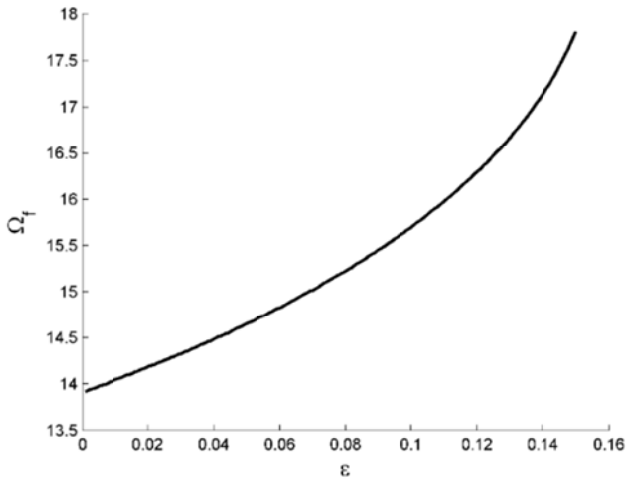


Figure 4: The flutter boundary vs. NES mass ratio.

Figure 5 presents the relationship between the flutter boundary and NES damping $\zeta$. It shows that increasing NES damping $\zeta$ would increase the flutter boundary of a rotating blade. The larger of NES damping, the more vibration energy would be dissipated.

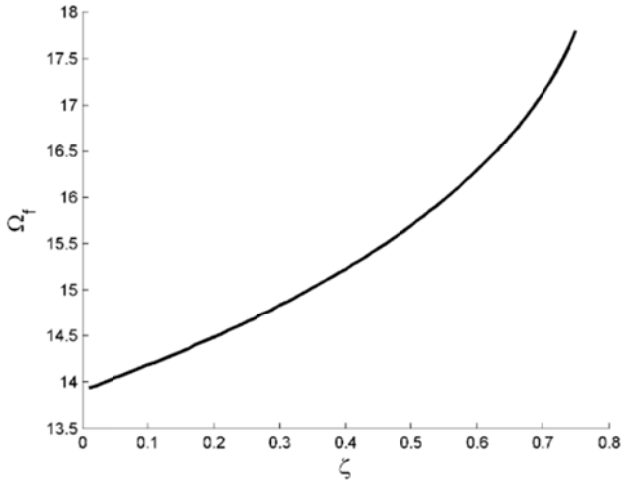


Figure 5: The flutter boundary vs. NES damping.

Figure 6 shows the relationship between the flutter boundary and NES position *d*. It shows that moving NES from the root to the end would increase the flutter boundary of a rotating blade. The reason is that vibration of rotating blade near the root is small, NES would absorb few vibration energy from the blade. When NES moves to the end of the blade, the vibration of rotating blade is large, and more vibration energy would be dissipated by NES.

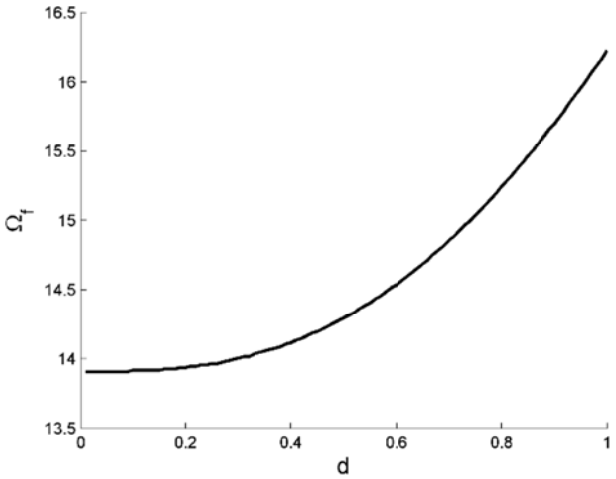


Figure 6: The flutter boundary vs. NES position.

More important, from (12), we can see that the nonlinear stiffness $\eta$ of NES is independent on the matrix B. It means that the flutter boundary of rotating blade is independent on $\eta$. Actually, the nonlinear stiffness is very important for vibration energy transmission between NES and rotating blade. Lee et al. [19] thought that the main role of the nonlinear stiffness is to provide broadband nonlinear resonant interaction between the primary and NES subsystems.

## 5. Conclusions

A NES is used to suppress the aeroelastic instability of a rotating blade under supersonic flow. The dynamic model of a rotating blade coupled with a NES is obtained. The Galerkin method is applied to discrete the nonlinear partial equations. Then, the dynamic responses of rotating blade are obtianed by numerical method. Results show that NES could mitigate the vibration of blade and change an aeroelastic instability blade to a stable blade. The flutter boundary of rotating blade is investigated by solving the eigenvalue problem. Increasing NES mass ratio or damping or moving NES to the end of the blade would increase the flutter boundary of rotating blade.

## Acknowledgement

This work is supported by the National Key Basic Research Program of China (No. 2015CB057400), National Natural Science Foundation of China (Grant No. 11302145), and Specialized Research Fund for the Doctoral Program of Higher Education (Grant No. 20130032120035).

## REFERENCES

1 Fazelzadeh, S. A. and Hosseini, M. Aerothermoelastic Behavior of Supersonic Rotating Thin-walled Beams Made of Functionally Graded Materials, *Journal of fluids and structures*, **23**(8), 1251-1264, (2007).

2 Fazelzadeh, S. A., Malekzadeh, P., Zahedinejad, P. and Hosseini, M. Vibration Analysis of Functionally Graded Thin-walled Rotating Blades Under High Temperature Supersonic Flow Using the Differential Quadrature Method, *Journal of sound and vibration*, **306**(1), 333-348, (2007).

3 Librescu, L. *Elastostatics and Kinetics of Anisotropic and Heterogeneous Shell-type Structures*. Springer Science & Business Media, (1975).

4 Oh, S. Y., Librescu, L. and Song, O. Thermoelastic Modeling and Vibration of Functionally Graded Thin-walled Rotating Blades, *AIAA Journal*, **41**(10), 2051-2061, (2003).

5 Oh, S. Y., Librescu, L. and Song, O. Vibration of Turbomachinery Rotating Blades Made-up of Functionally Graded Materials and Operating in a High Temperature Field, *Acta Mechanica*, **166**(1), 69-87, (2003).

6 Friedma, P. and Silverthorn, L. J. Aeroelastic Stability of Periodic Systems with Application to Rotor Blade Flutter, *AIAA Journal*, **12**(11), 1559-1565, (1974).

7 Friedmann, P. and Yuan, C. Effect of Modified Aerodynamic Strip Theories on Rotor Blade Aeroelastic Stability, *AIAA Journal*, **15**(7), 932-940, (1977).

8 Friedmann, P. and Robinson, L. H. Influence of Unsteady Aerodynamics on Rotor Blade Aeroelastic Stability and Response, *AIAA Journal*, **28**(10), 1806-1812, (1990).

9 Kim, T. and Dugundjit, J. Nonlinear Large Amplitude Aeroelastic Behavior of Composite Rotor Blades, *AIAA Journal*, **31**(8), 1489-1497, (1993).

10 Jeon, S. M., Cho, M. H. and Lee, I. Aeroelastic Analysis of Composite Rotor Blades in Hover, *Computers & Structures*, **66**(1), 59-67, (1998).

11 Sinha, S. K. Combined Torsional-bending-axial Dynamics of a Twisted Rotating Cantilever Timoshenko Beam with Contact-impact Loads at the Free End, *Journal of Applied Mechanics*, **74**(3), 505-522, (2007).

12 Hansen, M. H. Aeroelastic Instability Problems for Wind Turbines, *Wind Energy*, **10**(6), 551-577, (2007).

13 Pourazarm, P., Caracoglia, L., Lackner, M. and Modarres-Sadeghi Y. Stochastic Analysis of Flow-induced Dynamic Instabilities of Wind Turbine Blades, *Journal of Wind Engineering and Industrial Aerodynamics*, **137**, 37-45, (2015).

14 Pourazarm, P., Modarres-Sadeghi, Y. and Lackner, M. A Parametric Study of Coupled-mode Flutter for MW-size Wind Turbine Blades, *Wind Energy*, **19**(3), 497-514, (2016).

15 Vakakis, A. F., Gendelman, O. V., Bergman, L. A., McFarland, D. M., Kerschen, G. and Lee, Y. S. *Nonlinear Targeted Energy Transfer in Mechanical and Structural Systems*, Springer Science & Business Media, (2008).

16 Georgiades, F. and Vakakis, A. F. Dynamics of a Linear Beam with an Attached Local Nonlinear Energy Sink, *Communications in Nonlinear Science and Numerical Simulation*, **12**(5), 643-651, (2007).

17 Ahmadabadi, Z. N. and Khadem, S. E. Nonlinear Vibration Control of a Cantilever Beam by a Nonlinear Energy Sink, *Mechanism and Machine Theory*, **50**, 134-149, (2012).

18 Bab, S., Khadem, S. E., Mahdiabadi, M. K. and Shahgholi M. Vibration Mitigation of a Rotating Beam Under External Periodic Force Using a Nonlinear Energy Sink (NES), *Journal of Vibration and Control*, **23**(6), 1001-1025, (2015).

19 Lee, Y. S., Vakakis, A. F., Bergman, L. A., McFarland, D. M. and Kerschen, G. Enhancing the Robustness of Aeroelastic Instability Suppression Using Multi-Degree-of-Freedom Nonlinear Energy Sinks, *AIAA Journal*, **46**(6), 1371-1394, (2008).